Egyptian Journal of Chemistry

http://ejchem.journals.ekb.eg/

Thermal Shock Resistance for Binary $Al_{18}B_4O_{33}$ - Al_2O_3 Ceramic System via Solar and Electrical Energies

Sayed H. Kenawy [1,2*], Ahmed M. Khalil [3], Esmat M. A. Hamzawy [4]

[1] *Chemistry Department, College of Science, Imam Mohammad Ibn Saud Islamic University (IMSIU), Riyadh 11623, Saudi Arabia*
[2] *Refractories, Ceramics and Building Materials Department, National Research Centre, El-Buhouth St., Dokki - 12622, Giza, Egypt*
[3] *Photochemistry Department, National Research Centre, El-Buhouth St., Dokki - 12622, Giza, Egypt*
[4] *Glass Research Department, National Research Centre, El-Buhouth St., Dokki - 12622, Giza, Egypt*

Abstract

In the present work; the impact of the solar and electrical energy on microstructures, crystalline phases and mechanical properties in the binary aluminium borate/alumina ceramic composite, prepared by wet method were studied. Solar and electrical energy were employed by sintering the prepared samples at 1400 °C then thermally shocked at 1200°C and 1000°C in the 100 and 20 cycles respectively. Corundum (Al_2O_3) with a low content of aluminum borate ($Al_{18}B_4O_{33}$) was developed after sintering process and thermal shock. The scanning electron microscopy indicated a partial melting since the nano-scale rod crystals edges changed into curved one. Mechanical properties comprising (Young´s (E) and Coulomb´s (G) elastic moduli of elasticity) and density were investigated. The mechanical properties of these materials were deteriorated when compared with pure alumina ceramics. The flexural strength values of alumina ceramic showed the highest value of 244 MPa compared to 67 MPa for alumina/aluminum borate composite, after 100 cycles of thermal shock.

Keywords: Corundum; Aluminum borate ($Al_{18}B_4O_{33}$);Thermal shock; Nano-scale crystals

1. Introduction

Solar energy derived from the sun is the best source of sustainable energy on earth. Man has tended to exploit this energy in many uses and fields, including heating water and converting it into steam to generate electric energy, and from household uses, including heating or agriculture, solar panels to be applied in cooking [1]. Solar energy is a clean source of energy overcoming the environmental pollutants resulting from non-renewable energy sources such as fossil fuel. Due to the drastic increase in energy demand, recent researches have turned to the use of clean renewable energies, such as the heat of the solar, wind and tidal energies. These energies are able to be converted to distinct energies for various applications. Tuning some technologies can develop very high temperatures extending to several hundreds of degrees. Upon reaching these high temperatures, this clean energy can be applied in the field of ceramics, whether traditional or advanced ones. Regarding solar energy, it is found to be very cheap and maintains positive effects on the sintering processes of ceramic materials. Thus, it reduces the

production costs when utilized in industrialapplications [2].

Applying sun renewable energy in ceramic sintering as well as thermal shock is considered as promising modern trends accompanied by reducing the cost of advanced materials production. In some implementations, the high temperature resistance of ceramics is specifically important. For their catastrophe functions, the tolerance of such resistance is highly necessary. Various methods for evaluating how the ceramic material is sensitive to satisfy the expectations of different applications [3-6]. Mechanical stress is produced therein when ceramic load is applied to thermal cracking. Strain rate energy is needed upon exceeding the mechanical properties level, which is followed by the creation and propagation of cracks. It should be noted that SiC whiskers reinforced ceramic or metal matrix composites exhibit the desired options among all ceramic or metal matrix composite reinforcing fibers. This feature results from the improved characteristics of these whiskers. The high cost of the aforementioned whiskers, restricts the industrial use of the composites. New research has therefore

attempted to add low cost aluminum borate whiskers to the industrial application of composite metal matrix [7]. The cost of $Al_{18}B_4O_{33}$ is nearly 9% lower than the average SiC whisker. In addition, $Al_{18}B_4O_{33}$whisker possesses unique properties.They comprise high strength and Young's modulus (E) competing with those of SiC whisker [8].

Reinforced aluminum-based composites with borate whiskerswere investigated. A number of these compositeswas used in manufacturing carmotors [9-13]. It is substantial to evaluate their behavior at high-cycle surface temperatures and rapid cooling for so-called advanced technical ceramics. When the sample is thermally treated, variations in temperature exists between its top and its interior matrix, which is a highly mechanical stress. This kind of stresses can cause preexisting defects to develop with the consequent degradation inits properties. Some studies showed alterations in alumina behavior when subjected to thermal shock [14-18]. We are not sure about certain experimental studies that expose the behavior of aluminum borate/alumina when subjected to cycles of high surface temperatures and cooling fast.

The main objective of this work was to evaluate the behavior of aluminum borate/alumina when subjected to rapid solar thermal shock cycles of temperature variation compared with conventional thermal shock using electrical furnace.

2. Materials and methods
2.1. Materials
The present composite materials were composed of α-alumina as matrix. Moreover, pre-prepared aluminum borate is a reinforcing material. Alumina source was submicron α-alumina (Boehringer Ingelheim Chemicals Japan). Its particle sizes and surface area of alumina powder were within the range of 0.22-0.27 μm and 14-15 m^2/g, respectively. In addition, aluminum borate nano-fibers are used as reinforcing materials. On the other side, the aluminum borate nano-fibers were synthesized using bauxite raw material (SiO_2 : 13.32% ; Al_2O_3 : 79.13% and TiO_2 : 3.59 %. Fe_2O_3 : 2.83%; Na_2O+K_2O : 0.40%.$CaO+MgO$: 0.24% ; ZrO_2 : 0.11% , P_2O_5 : 0.16%) and boric acid (H_3BO_3) to design $Al_{18}B_4O_{33}$ [3].

2.2. Preparation of the composites

The preparation of aluminum borate nano-fibers was based on introducing (H_3BO_3) in wt. % of 5, 10, 15, 20 and 25 g with respect to 100 g of bauxite. In order to obtain homogenous, finely dispersed and un-agglomerated mixtures; Al_2O_3/aluminum borate mass ratios were (95/5, 90/10 and 85/15). Then, they were milled for 24 h in a ball mill containing 150 ml ethanol together with 50 g

Al_2O_3 balls as demonstrated in Table 1. For preparing the composite samples, the admixed sample powders (0.053 mm) were casted. They were placed in discs of volume (3 x 0.3 cm^3) at 25 KN. PVA (7%) in aqueous solution was employed as binder. The firing process was conducted up to 1450 °C using a rate of heating of 5 °C/min. The discs were fired within 1000 to 1500 °C temperature ranges. The microcrystalline structure was examined by scanning electron microscope SEM/EDX with attached energy dispersive X-ray spectrometer (SEM Model Quanta 250, Holland).
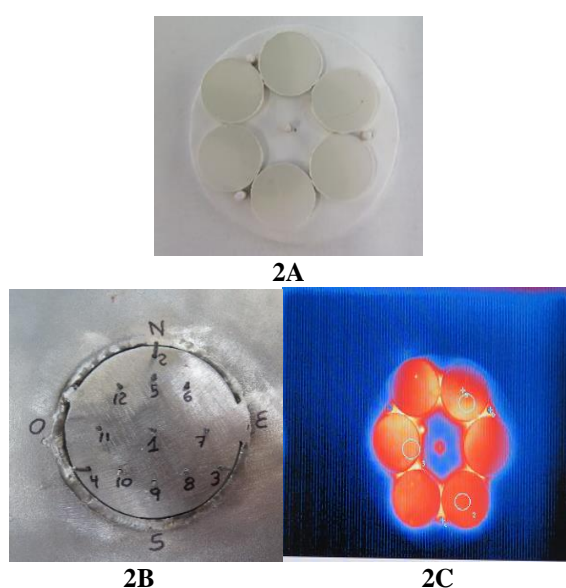
For thermal shock tests, both controlled solar energy and electrical furnace were used. The source of controlled solar energy consists of 130 m^2 flat heliostat placed on the outside of the building and a concentrator with about 100 m^2 of reflection surface as shown in Fig. 1. The power rating of this oven is close to 69 kW. Fig. 2 explains the experimental arrangement (positioning of test pieces and thermocouples).It was used to expose aluminum borate/alumina into concentrated solar radiation. In Fig. 2A, 6 discs of aluminum borate/alumina positioned on a zirconia felt, with 5 cm diameter/disc.Then, they wereset to besubjected to concentrated solar irradiation. Beneath each specimen, there are Pt/Rd thermocouples to ensure the isothermal heating of the samples as displayed in Fig. 2B. To assure the mechanical properties results, identical test specimens were subjected to thermal cycling in groups of 3x6 =18 test pieces. Fig. 2C shows the temperature distribution to be evaluated through an infrared camera (IR CAM) and specific software of analysis.
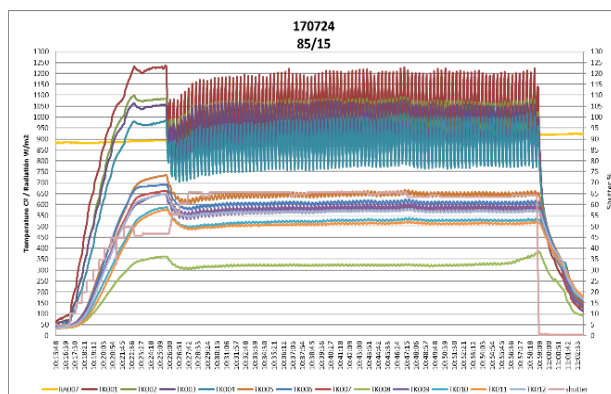

Fig. 1. Aspect of the parabolic concentrator and the test platform (with mirror reflector inclined at 45 degrees) of the oven SF60 of the Solar Platform of Almeria.

In order to obtain the rapid heating-cooling cycles, an automated system has been set: a shuttle-type bulkhead, which alternately allows return the solar radiation to be cut and reset before it reaches the focal zone, where the test pieces are placed. The cooling of the test pieces can be accelerated by the application of surrounding air. All tested specimens through solar energy were subjected to 100 cycles of

temperature variation through a maxima of T_{max} = 1200 °C.The readings were recorded by thermocouple number 1 (thermocouple central). Some differences between treatments of the three groups of specimens were submitted and given in. Moreover, the samples subjected to thermal shock through electrical furnace at 1000°C for 20 cycles were characterized by X-ray diffraction and SEM / EDX analysis. Fig. 3 demonstrates an example of the heating-cooling cycles. The cycles are correlated to the test specimens of alumina/aluminium borate samples. The surrounding conditions were ($T_{max} \approx$ 1200°C; $T_{min} \approx 700$ °C). The 6 discs were subjected to 100 cycles. The temperature indicated in Fig. 3 is the recorded one by the thermocouple located in the center (denoted with the number 1 in Fig. 2B).

2A

2B   **2C**

Fig. 2. Photos showing the experimental arrangement of the samples in the focal zone: A) positioning of thetested pieces aluminum borate/alumina discs); B) positioning of the tip of the thermocouples and C) IR Camera for temperature distribution.

Fig. 3. A model graph presenting the data recorded during a thermal-cycling test.

3. Results and Discussion

Two routes for designing and choosing materials to achieve high thermal shock are commonly available [19]. Avoiding the initiation of fissures initiation is the first route. The second one is to monitor the cracks are propagated. The desired material properties comprise the high strength and thermal conductivity. Moreover, the low thermal expansion coefficient may prevent the resulting crack from the thermal shock. Two main types of high Tc ceramics exist. The first type shows high strength and thermal conductivity. The second one has a low thermal expansion coefficient [20]. Resisting the thermal shock may be enhanced by the improvement of σ. Moreover, bending strength, Young's modulus and α coefficient of thermal expansion are considered. Hence, without developing creep, the matrix may be encounter thermal stresses. Porosity is suggested to have a negative influence on ceramics' cold-shock resistance, but it possesses a beneficial effect to hot-shock resistance [21]. However, Young's modulus (E) can be diminished by the pores in ceramics. These pores contain gases. Usually, they are not affected by thermal expansion coefficient [19]. During thermal shock, some thermo-mechanical properties alter.They comprise cracking, tensile stresses during posterior thermal shocks. Some changes may arisein the structure of the residual glass phase.They indicate the formation of more liquid phase in addition to much α SiO2 formation. Thus, weakening the material. Moreover, residual bending power arise.The lattercounters the enhancement of thermal shock resistance. The pre-sintered sample's thermal shock (1450 °C/2h) at 1000 °C for 20 times displays no change in the sample surface. The sintered casted samples show the crystallization of corundum (α-Al_2O_3, ICCD 46-1212). In addition, a very little amount of aluminum borate was developed too ($9Al_2O_3.2B_2O_3$, ICDD 80-2301). Before and after thermal shock (at 1000 °C for 20 cycles), corundum was developed in all the samples,however aluminum borate was developed in AB10 and AB15 samples as shown in Fig. 4.

Table 1. Composition of the binary alumina and the pre prepared aluminum borate.

Sample	Composition	
	Submicron α-alumina in mass%	$Al_{18}B_4O_{33}$ whiskers in mass%
A	100	0%
AB5	95	5%
AB10	90	10%
AB15	85	15%

The dominance of corundum as the main phase represents the high alumina to boron oxide ratio. The performed measurements made allowed the value of the studied properties to be known before and after the test pieces were subjected to thermal cycles. This was the used technique upon exposure to high temperature cycles to determine the potential deterioration of the material. Table 2 summarizes the results of the experimental determination of the following properties of aluminum borate/alumina composites. They are density (according to Archimedes principle; Young's elastic modulus (E); Coulomb elastic modulus (G) and flexural strength. The values in Table 2 are accompanied by the respective values of the standard deviation.

This work allowed us to demonstrate the work with regard to the possibility of executing rapid cycles of temperature variation through the current high concentration solar furnaces; and the conductivity of the tested material: aluminum borate/alumina. This work proved to be of the same good quality. They do not show rupture in any of the tested pieces upon exposing them to temperature cycles. The different sequences of 100 cycles (even the faster and more drastic sequence of 100 cycles in 77 minutes (T_{max} = 1200 °C and T_{min} = 400 °C) did not display significant changes in any of the evaluated properties. The latter ones comprise density, Young's modulus, Coulomb modulus and flexural strength. The aforementioned properties were monitored before and after the application of the heating-cooling. The detected variation is practically negligible. It consisted of decaying the flexural strength after the application of 100 cycles in 150 minutes. The temperature was T_{max} = 1200 °C and T_{min} = 400 °C. Primarily, the value was 244 (± 46) MPa. After these 100 cycles, it became 211 (± 34) MPa.
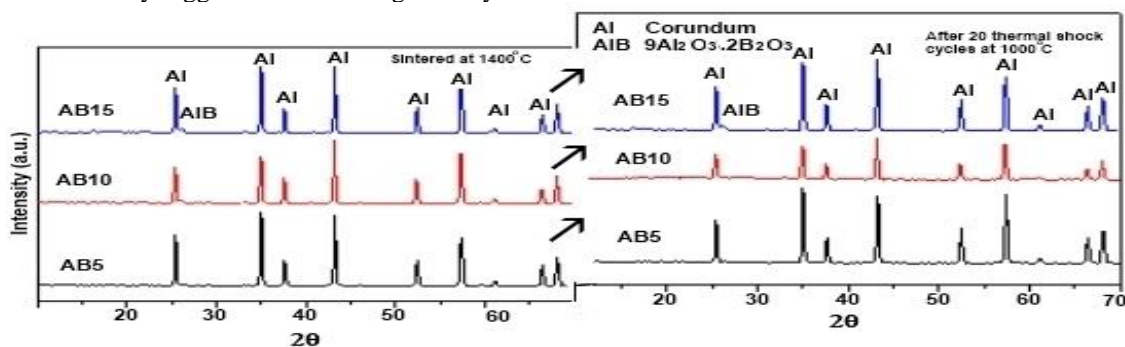
SEM micrographs for the ceramic samples before and after thermal shock cycles are shown in Fig. 5. All the samples demonstrate rod-like crystals near one micron or in nano-scales. The rod thickness was between 100 and 500 nm. Generally, in looking to microstructure, after thermal shock the samples become relatively bigger with round edges. Only the

AB10 sample (3B) does not show significant changes in the rod size (Fig. 4). This was relevant to the microstructure of fine aluminum borate whiskers. The falling trend of the hardness value may be related to the larger crystal size. In particular, large internal stresses and micro-cracks along the tubes upon indentation may have been caused by the creation of hollow tubes. This led to simple crack propagation routes. The interlocking microstructure resulted in higher hardness in samples with smaller whisker crystals randomly targeted [22]. An inconsiderable fluctuation occurred in accordance with the changing phase. It may be the reason for which the starting raw materials were mixed heterogeneously.

Moreover, the placed sample at different furnace locations may lead to diversified temperatures. The lost bending strength rates of AB5, AB10, AB15 and AB20 vary as follows:
1-12 %, 13-21 %, 2-19 % and 11-28 % respectively. They start from their zero period values. For more than 30 times of thermal shock, the surfaces of the samples did not exhibit cracks.

The dispersion nature of ceramics may be the probable explanation. Changing the pressure or the holding time should exist for each sample. On the other hand, different temperatures could be another explanation for coming from different locations of one furnace. After 30 times of thermal shock, no changes in the crystal phase can be observed. The surface of the samples did not change prior to and after being thermally shocked. The lost bending strength rate can increase directly proportional with thermal shock times. The glass and crystal phase thermal expansion coefficient vary. Mullite and cordierite will show a relaxing thermal expansion. This feature takes place as the stress at the interface of micro-cracked exists with toughening the composite ceramic. The presence of nano-rod may assist in the thermal shock resistance. It augments here as the existing nano-rod supplies a wavy fractured surface. The latter magnifies the area and toughness of the fractured plane [23]. Several pellets exist around or above the nano-rods.
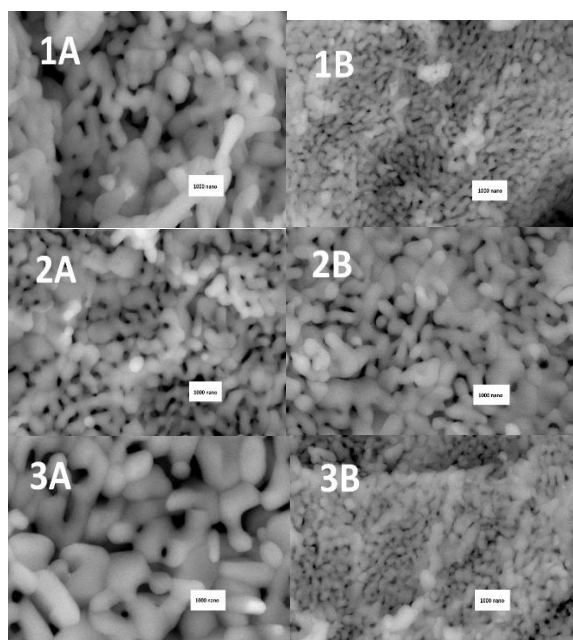

Fig. 4. X-ray diffraction patterns of sintered ceramic (at 1400 °C/2h) samples before and after thermal cycles at 1000 °C.

Table 2. Mean value (± standard deviation) before and after the cycles for the properties of both alumina and aluminium borate/alumina composites.

| Sample | Thermal Shock | | | Properties | | | | |
	Temp. °C	No. of cycles	Time min.	Density kg/m^3	E MPa	G MPa	Poisson's ratio	Flexural StrengthMPa
A	--	--	--	3.90-3.94	355-376	154-161	0.15	244±46
A	1200-900	100	35	3.92- 3.95	357-378	154-161	0,16	238 ± 37
A	1200-900	100	150	3.92 - 3.95	354 - 369	154-160	0,16	244±31
A	1200-900	100	77	3.89 - 3.94	354 - 369	154-161	0.15	242 ± 31
AB5	--	---	--	2.37 - 2.67				28 ± 15
	1200-900	100	35	2.34 - 2.62				28 ± 15
AB10	--	--	--	3.32 - 3.49				67 ± 14
	1200-900	100	35	3.22 - 3.49				63 ± 26
AB15	--	--	--	3.22 - 3.40				37 ± 9
	1200-900	100	35	3.26 - 3.33				23 ± 8

It is postulated that the facets of these rods surface are sufficiently efficient to pull each other. Alternatively, the thermal shock resistance at 1100ºC for 20 minutes can explain the growth of the mullite crystal along the way. However, the micro-cracks spread across the broad crystal borders. The highest residual strength ratio arises beyond a 30 fold period. Surplus cracks may emerge due to the thermal stresses that arose at higher quenching cycles [24].

Fig. 5. SEM micrographs of the ceramic samples before (1A, 2A and 3A) and after (1B, 2B and 3B) thermal shock cycles at 1000 °C.

It has been demonstrated that the apparent porosity increases with the growth of whisker content at the same sintering temperature. This is due to the aluminum borate whisker's melting point is 1440 °C. At higher sintering temperature, the whiskers possess anelevated creep resistance. Excessive whiskers would thus impede the shrinkage with a densification in the matrix of aluminum phosphate [25]. The increment in the density may due to the partial melting of AlBO whiskers forming a glassy phase which leads to decreasing the porosity.

4. Conclusions

In summary, various ceramics materials of binary aluminum borate/alumina composite were successfully produced using facile wet chemical precipitation method. The thermal shock was carried out using both solar and electrical furnace for comparison. The samples were thermally shocked at 1200 °C and 1000 °C in the 100 and 20 cycles respectively. The SEM investigation illustrated that alumina phase with a low content of aluminum borate after thermal shock did not show any cracks. The mechanical properties displayed the highest value of 244 MPa for alumina ceramics as compared with alumina/aluminum borate composite of 67 MPa after 100 cycles of thermal shock.

Acknowledgements

_____

Conflicts of Interest

The authors declare no conflict of interest.

References

1. H. El Ghetany, W. I. Aly, H. A. Shalata, A. I. Eid, K. Abdelwahed, Experimental investigation of an energy saving system using Phase Change Materials in buildings. Egy. J. Chem. 63 (11) (2020) 4533-4545. https://doi:10.21608/EJCHEM.2020.27252.2565

2. S. Guillot, A. Faik, A. Rakhmatullin, J. Lmbert, E. Veron, P. Echegut, C. Bessada, N. Calvet, X. Py, Corrosion effects between molten salts and thermal storage material for concentrated solar power plants, Appl. Energy. 94 (2012) 174-181. https://doi:10.1016/j.apenergy.2011.12.057

3. S. H. Kenawy, W. M. N. Nour, Microstructural evaluation of thermally fatigued SiC-reinforced Al2O3/ZrO2 matrix composites, J. Mater. Sci. 40 (2005) 3789-3793. https://doi:10.1007/s10853-005-3320-x

4. S. H. Kenawy, A. M. Khalil, Advanced ceramics and relevant polymers for environmental and biomedical applications, Biointerface Res. Appl. Chem. 10 (2020) 5747-5754. https://doi.org/10.33263/BRIAC104.747754

5. M. A. El-Khateeb, S. H. Kenawy, A. M. Khalil, F. A. Samhan, Polishing of secondary treated wastewater using nano-ceramic hybrid PET waste plastic sheets, Desalin. Water Treat. 217 (2021) 214-220. https://doi:10.5004/dwt.2021.26847

6. A. M. Khalil, S. H. Kenawy, Hybrid membranes based on clay-polymer for removing methylene blue from water, Acta Chim. Slov. 67 (1) (2020) 96-104.http://dx.doi.org/10.17344/acsi.2019.5227

7. S. H. Kenawy, Synthesis and Characterization of Aluminum Borate Ceramic Whiskers, Int. J. Appl. Ceram. Technol. 8 (2011) 783-792. https://doi:10.1111/j.1744-7402.2010.02505.x

8. G. Zhang, J. H. Yang, In Situ Synthesis Aluminum Borate Whiskers Reinforced TiB$_2$ Matrix Composites for Application in Aluminum Reduction Cells, JOM. 65 (2013) 1467-1471. https://doi:10.1007/s11837-013-0710-4

9. Z. Chang, Y. Wu, T. Iizuka, L. Peng, W. Ding, High-strength and high-modulus Al$_{18}$B$_4$O$_{33}$W/GWZ1031K magnesium matrix composite prepared by squeeze casting, Mater. Sci. Eng. A. 817 (2021) 141393. https://doi:10.1016/j.msea.2021.141393

10. R. A. Hamza, K. A. Samawi, Taghried Salman, Inhibition Studies of Aluminium alloy, (2024) Corrosion in Acid Hydrochloride Solution Using an Expired Phenylphrine Drug, Egy. J. Chem. 63 (8) (2020) 2863-2875. https://doi:10.21608/EJCHEM.2020.19583.2222

11. L. J. Yao, G. Sasaki, J. Pan, M. Yoshida, H. Fukunaga, Effect of interfacial reaction on bending strength of Al$_{18}$B$_4$O$_{33}$ whisker-reinforced aluminum composites, Metall. Mater. Trans. A. 29 (1998) 1517-1524.

12. D. Y. Ding, D. Z. Wang, C. K. Yao, Control of the interfacial reaction in aluminum borate whisker-reinforced 6061Al composite by sol-gel alumina coating, J. Mater. Sci. Lett. 18 (1999) 569-570. https://doi:10.1023/A:1006690931629

13. D. Grossin, A. Monton, P. Navarrete-Segado, E. Ozmen, G. Urruth, F. Maury, D. Maury, C. Frances, M. Tourbin, P. Lenormand, G. Bertrand, A review of additive manufacturing of ceramics by powder bed selective laser processing (sintering/melting): Calcium phosphate, silicon carbide, zirconia, alumina, and their composites, Open Ceram. 5 (2021) 100073. https://doi:10.1016/j.oceram.2021.100073

14. M. Saadaoui, G. Fantozzi, Crack growth resistance under thermal shock loading of alumina, Mater. Sci. Eng. A. 247 (1998) 142-151. https://doi:10.1016/S0921-5093(97)00768-5

15. A. Yahya, B. El-Kalioby, A. M. Soltan, S. K. Ibrahim, E. Hamzawy, Cordierite ceramic through glass and ceramic routes from kaolin and talc. Egy. J. Chem. 64 (4) (2021) 1751-1758. https://doi:10.21608/EJCHEM.2021.53853.3115

16. Y. Luo, H. Gu, M. Zhang, A. Huang, H. Li, C. Yu, T. Li, P. Yan, Research on thermal shock resistance of porous refractory material by strain-life fatigue approach, Ceram. Int. 46 (2020) 14884-14893. https://doi:10.1016/j.ceramint.2020.03.015

17. H. Belghalem, M. Hamidouche, L. Gremillard, G. Bonnefont, G. Fantozzi, Thermal shock resistance of two micro-structured alumina obtained by natural sintering and SPS.Ceram. Int.40 (2014) 619–627. https://doi:10.1016/j.ceramint.2013.06.045

18. D. Li, W. Li, W.G., R. Wang, H. Kou, Influence of thermal shock damage on the flexure strength of alumina ceramic at different temperatures, Mater. Lett.173 (2016) 91-94.https://doi:10.1016/j.matlet.2016.03.026

19. M. Dimitrijevic, M. Posarac, R. Jancic-Heinemman1 ,J. Majstorovic , T. Volkov-Husovic, B. Matovic, Thermal shock resistance of ceramic fibre composites characterized by non-destructive methods, Process. Appl. Ceram.

_____

2 (2008) 115-119. https://doi:10.2298/PAC0802115D

20. D. Li, Z. Yangn, D. Jian, D. Wu, Q. Zhu, B. Liang, S. Wang, Y. Zhou, Microstructure, oxidation and thermal shock resistance of graphene reinforced SiBCN ceramics, Ceram. Int. 42 (2016) 4429-4444. https://doi:10.1016/j.ceramint.2015.11.127

21. P. Sooksaen, Structure and Crystallization of Borate-Based Glasses for Machinable Material Applications, Int. J. Appl. Phys. Math. 2, (2012) 89-92. https://doi:10.7763/IJAPM.2012.V2.60

22. S. H. Kenawy, E. M. A. Hamzawy, Negative thermal expansion occurs in a bauxite-based aluminum borate ceramic whisker with nanofibers microstructure. Metall. Mater. Trans. A. 49 (2018) 4980-4985. https://doi:10.1007/s11661-018-4739-4.

23. A. A. Rubinstein, Crack-path effect on material toughness, J. Appl. Mech. (1990): 57 (1990) 97-103. https://doi:10.1115/1.2888331

24. X. Xiaohong, M. Xionghua, W. Jianfeng, C. Ling, X. Tao, Z. Mengqi, *In-Situ* Preparation and Thermal Shock Resistance of Mullite-Cordierite Heat Tube Material for Solar Thermal Power, J. Wuhan Univ. Technol. Mater. Sci. Ed. 28 (2013) 407-412. https://doi:10.1007/s11595-013-0704-7

25. Z. Lu, H. Geng H., M. Zhang, X. Hou, Preparation of aluminum borate whisker reinforced aluminum phosphate wave-transparent materials, Chin. Sci. Bull. 53 (2008) 3073-3076. https://doi:10.1007/s11434-008-0433-z